Critical Structure-Function Determinants within the N-Terminal Region of Pulmonary Surfactant Protein SP-B

Alicia G. Serrano,* Marnie Ryan,† Timothy E. Weaver,† and Jesús Pérez-Gil*
*Departamento de Bioquímica y Biología Molecular I, Facultad de Biología, Universidad Complutense, Madrid, Spain; and
†Division of Pulmonary Biology, Cincinnati Children's Hospital Medical Center, and University of Cincinnati, Ohio

ABSTRACT Surfactant protein SP-B is absolutely required for the surface activity of pulmonary surfactant and postnatal lung function. The results of a previous study indicated that the N-terminal segment of SP-B, comprising residues 1–9, is specifically required for surface activity, and suggested that prolines 2, 4, and 6 as well as tryptophan 9, may constitute essential structural motifs for protein function. In this work, we assessed the role of these two motifs in promoting the formation and maintenance of surface-active films. Three synthetic peptides were synthesized including a peptide corresponding to the N-terminal 37 amino acids of native SP-B and two variants in which prolines 2, 4, 6, or tryptophan 9 were substituted by alanines. All three synthetic peptides were surface-active, as expected from their amphipathic structure. The peptides were also able to insert into dipalmitoylphosphatidylcholine/palmitoyloleoylphosphatidylglycerol (7:3 w/w ratio) monolayers preformed at pressures >30 mN/m, indicating that they perturb and insert into membranes. Substitution of alanine for tryptophan at position 9 significantly decreased both the rate of adsorption/insertion of the peptide into the interface and reinsertion of surface-active material excluded from the film during successive compression-expansion cycles. Substitution of alanines for prolines at positions 2, 4, and 6 did not produce substantial changes in the rate of adsorption/insertion; however, reinsertion of surface-active material into the expanding interface film was not as effective as in the presence of the nativelike peptide. These results suggest that W9 is critical for optimal interface affinity, whereas prolines may promote a conformation that facilitates rapid insertion of the peptide into phospholipid monolayers compressed to the highest pressures during compression-expansion cycling.

INTRODUCTION

Surfactant protein B (SP-B), a very hydrophobic polypeptide of 79 amino acids, plays a critical role in the organization and function of pulmonary surfactant (1). Surfactant is a lipid-protein complex secreted by type II pneumocytes into the thin aqueous layer that covers the alveoli where it spontaneously adsorbs to the air-water interface. The surfactant film reduces surface tension to values close to 0 mN/m at end expiration, thereby preventing alveolar collapse. The lipid fraction of surfactant, which contains ~40% dipalmitoylphosphocholine (DPPC) and 10% phosphatidylglycerol (PG), is directly responsible for the surface-active function; however, efficient formation and maintenance of a surfactant film during successive compression-expansion cycles requires the presence of SP-B or another hydrophobic surfactant protein, SP-C. Genetic deficiency of SP-B in both humans and mice causes lethal respiratory failure at birth (2,3), demonstrating that this peptide is absolutely required for lung function. In contrast, genetic deficiency of SP-C in mice is not associated with neonatal respiratory failure (4).

Premature infants presenting with lung immaturity often develop neonatal respiratory distress syndrome arising from surfactant deficiency, elevated surface tension, and alveolar collapse. Prompt treatment with an exogenous surfactant preparation containing surfactant lipids and SP-B and/or SP-C can rapidly restore lung function in premature infants. SP-B is required for postnatal lung function and survival (5,6) and SP-B concentration is decreased in some patients with acute respiratory distress syndrome (7). Therefore, it can be anticipated that SP-B, or a functional analog of the protein, will be an important component of a surfactant therapy for treatment of acute respiratory distress syndrome. Because there is currently no expression system capable of producing a recombinant peptide similar to native SP-B, a detailed study of the structure-function relationships of the protein is important to define the minimal structural determinants able to mimic SP-B functions in a synthetic peptide.

SP-B is isolated from alveolar airspaces as an homodimer that is stabilized by an intermolecular disulphide bridge. Three intramolecular disulphide bridges are present in each monomer, revealing the disulphide bond pattern typical of all saposin-like proteins (8). Members of this family include amoebapores, sulphated glycoprotein-1, acyloxyacylhydrolase, acid sphingomyelinase, the sphingolipid-activating proteins (saposins), and NK-lysin, for which the three-dimensional structure has been determined by NMR (9). All of these proteins transiently interact with lipids but their functions in vivo are quite varied. SP-B is very hydrophobic, and is the only saposin-like protein that is always lipid-associated. The structure and lipid binding properties of SP-B have been extensively studied using different techniques (10–13). Although the three-dimensional structure of SP-B is still not known, several studies have suggested that SP-B interacts

Submitted August 26, 2005, and accepted for publication September 27, 2005.

Address reprint requests to Jesús Pérez-Gil, Departamento de Bioquímica, Facultad de Biología, Universidad Complutense, 28040 Madrid, Spain. Tel.: 34-91-394-4994; Fax: 34-91-394-4672; E-mail: jpg@bbm1.ucm.es.

0006-3495/06/01/238/12 $2.00

doi: 10.1529/biophysj.105.073403

with lipids via four or five amphipathic α-helices (14,15). This interaction leads to fusion and lysis of lipid vesicles (16–18), activities that might be critical for packaging of surfactant phospholipids in the exocytic pathway of type II pneumocytes. SP-B-mediated fusion and lysis may also play an important role in the formation and maintenance of the surface film and the closely linked reservoir of surfactant material extended underneath (19). The potential importance of these particular SP-B properties in surfactant membrane transitions has recently been addressed by Ryan and coworkers (20). Synthetic peptides were used to map the fusogenic and lytic activities of the protein, and assess the requirement of these properties for SP-B surface activity. The results suggested that the fusogenic, lytic, and surface activities of SP-B mapped predominantly to the N-terminal half of the protein (residues 1–37) and that decreased lytic or fusogenic activities were associated with altered surface properties of the peptide. The N-terminal segment (residues 1–9), which played little or no role in membrane fusion or lysis, appeared to be critical for the surface-tension-reducing properties of SP-B: Substitutions in the N-terminal segment (tryptophan 9 or prolines 2, 4, and 6) critically inhibited the surface activity without affecting liposome fusion or lysis. In this work, we have analyzed the role of the N-terminal motif in the formation and maintenance of surface-active films subjected to dynamic compression-expansion cycling.

MATERIALS AND METHODS

Materials

Chloroform and methanol were HPLC-grade solvents from Scharlau (Barcelona, Spain). Phospholipids 1,2-dipalmitoyl-*sn*-glycero-3-phosphocholine (DPPC) and 1-palmitoyl-2-oleoylphosphatidylglycerol (POPG) were from Avanti Polar Lipids (Birmingham, AL). Synthetic peptides were designed to mimic the native sequence or two variants of the N-terminal half of SP-B (residues 1–37) (Fig. 1), which contains most determinants for SP-B-promoted membrane-perturbation and surface activity (20). The peptides were synthesized by Biosynthesis (Lewisville, TX) by F-moc chemistry and purified to >95% homogeneity by HPLC. Peptide composition was confirmed by mass spectrometry. All other reagents and chemicals were purchased from Merck (Darmstadt, Germany).

Circular dichroism

Far-UV circular dichroism (CD) spectra were recorded as previously described (21) in a Jasco 715 spectropolarimeter equipped with a Xenon lamp. All spectra were recorded in a 0.2-mL thermostated quartz cell with an optical path length of 0.1 cm. Molar ellipticity was calculated taking 110 as the mean molecular weight per residue. Estimation of the secondary structure content from the CD measurements was performed after deconvolution of the experimental spectra into four simple components (α-helix, β-sheet, turns, and random coil) using the CDPro software package containing three commonly used programs: SELCON3, CONTIN/LL, and CDSSTR (22,23). This software allows the use of different sets of proteins, including membrane proteins (SMP50), to increase the reliability of the analysis in the case of the membrane-interacting SP-B peptides.

Intrinsic fluorescence of SP-B synthetic peptides

Tryptophan fluorescence emission spectra of SP-B synthetic peptides in methanol were recorded in a SLM-Aminco AB-2 spectrofluorimeter at 25°C. Peptide concentration was 10 μg/mL. Excitation wavelength was set at 275 or 290 nm, and emission spectra were measured over the range of 290–430 nm. Both excitation and emission slits were set at 4 nm and the cell path was 0.2 cm. The contribution of tyrosine to the emission spectra was calculated, as described elsewhere (24), by subtracting from the emission spectra measured exciting at 275 nm, the emission spectra obtained exciting at 290 nm multiplied by a normalizing factor. This factor is the ratio between the fluorescence intensities measured using excitation at 275 nm and 290 nm, respectively, at emission wavelengths higher than 380 nm, where no Tyr contribution is expected.

Interfacial adsorption of peptides

Interfacial adsorption of SP-B synthetic peptides was assayed using a specially designed surface balance previously described (25). The microbalance was filled with 1.5 mL of buffer (Tris 5 mM, NaCl 150 mM, pH 7) and, after 5-min equilibration, 10 μL of methanol containing different amounts of SP-B synthetic peptides was injected into the subphase. Changes in surface pressure (π) were then monitored over time. The subphase was continuously stirred and the trough was thermostated at 25°C. Subphases were prepared with double-distilled water (the second distillation performed in the presence of potassium permanganate). Injection of equivalent volumes of pure methanol did not produce any detectable change in surface pressure.

Insertion of peptides into preformed monolayers

Insertion of SP-B synthetic peptides into phospholipid monolayers, preformed at different initial surface pressures (π_i), was followed (using the same microbalance) by monitoring changes in surface pressure ($\Delta\pi$) over time, after peptide injection into the subphase (Tris 5 mM, NaCl 150 mM, pH7). Subphases were prepared with double-distilled water (the second

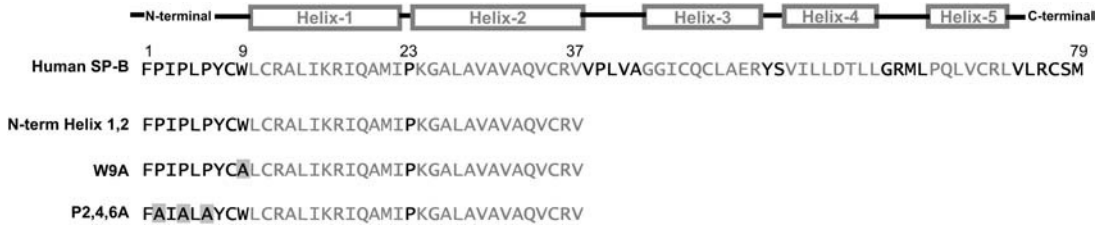

FIGURE 1 Sequence of SP-B-derived peptides. Amino-acid sequence of human SP-B and the SP-B-derived synthetic peptides studied in this work. Shaded boxes represent proposed helical regions, and black lines the predicted interhelical loops derived by fitting the sequence of the SP-B mature peptide to the three-dimensional structure of NK-lysin (9). Amino-acid substitutions in the variant synthetic peptides appear shaded. Note that the exact boundaries of these domains remain unclear.

distillation performed in the presence of potassium permanganate). Phospholipid monolayers were preformed by spreading a concentrated solution of the lipids (DPPC/POPG, 7:3, w/w) in chloroform/methanol (3:1, v/v) on top of the aqueous surface. After 10-min stabilization, 4 μL (1 mg/mL) of peptide in methanol were injected into the subphase. The highest increment in surface pressure ($\Delta\pi$) was plotted versus the initial pressure (π_i), allowing calculation of the critical insertion pressure (π_c), defined as the maximum π at which the peptide can still insert. The subphase was continuously stirred and the temperature was kept constant at 25°C during the experiment.

π-*A* isotherms of lipid and lipid/peptide monolayers

Monolayers of lipid (DPPC/POPG, 7:3, w/w) or lipid/peptide binary systems were made by spreading 33 μL of a concentrated lipid or lipid/peptide solution in chloroform/methanol (3:1, v/v) at the surface of a 5 mM Tris buffered subphase, pH 7, containing 150 mM NaCl. These monolayers were prepared as previously described (25), in a thermostated (25°C) Langmuir-Blodgett trough (NIMA Technologies, Coventry, United Kingdom) equipped with a ribbon barrier to minimize film leakage during compression. Subphases were prepared with double-distilled water (the second distillation performed in the presence of potassium permanganate). After spreading the sample on top of the subphase, the organic solvent was allowed to evaporate for 10 min before starting compression. The total area of the interface was 225 cm^2 and the monolayer was compressed at 65 cm^2/min, while changes in surface pressure (π), measured with a Wilhelmy dipping plate of Whatman No. 1 paper attached to the pressure transducer, were recorded and plotted against the area occupied per phospholipid molecule (*A*).

To analyze the effect of the SP-B synthetic peptides during successive compression-expansion cycles, monolayers prepared as described above were compressed and expanded at 65 cm^2/min, up to four cycles, while surface pressure-area (π-*A*) data were collected.

Statistics

Unless otherwise indicated, the results are presented as representative experiments after repeated examination of three different samples.

RESULTS

Structure of SP-B synthetic peptides

The secondary structure of SP-B synthetic peptides in methanol was analyzed by CD spectroscopy. Fig. 2 shows the far-UV CD spectra of three SP-B synthetic peptides (N-term Helix 1,2, W9A, and P2,4,6A) containing the amino-acid sequence of the N-terminal half of SP-B with or without the substitutions indicated in Fig. 1. All the spectra exhibited CD features consistent with a mainly α-helical conformation, including ellipticity minima at 208 and 222 nm and a marked maximum at 195 nm. Analysis of the experimental data, using the CDPro suite of programs (SELCON3, CONTIN/LL, and CDSSTR) (22,23), allowed estimation of relative proportions of different types of secondary structure. Table 1 shows that peptide N-term Helix 1,2 contained ~45% α-helix, whereas peptides W9A and P2,4,6A contained ~55% α-helix. The proportion of helical structure was lower than predicted by the model in Fig. 1, perhaps reflecting the higher intrinsic flexibility of peptides compared to the disulfide-linked structure of NK-lysin or SP-B. Another possibility is that amino acids 26–37 could adopt a β-sheet conformation in at least a fraction of the peptide, as has been suggested with other synthetic peptides of this region of SP-B (26). More insight into the three-dimensional structure of the two peptides containing tryptophan, the main residue responsible for the intrinsic fluorescence of proteins, was obtained from the fluorescence emission spectra of methanolic solutions of N-term Helix 1,2 and P2,4,6A peptides (Fig. 3). Fluorescence-emission maximum was centered at 335 nm in both cases, ~15 nm below the wavelength of the maximum fluorescence expected for free tryptophan in aqueous solution (~350 nm) (27). The contribution of Tyr to the total fluorescence spectrum obtained by excitation at 275 nm was higher in the case of P2,4,6A peptide than in the case of the peptide with the native sequence, indicating that the distance and/or the orientation of the two aromatic residues might have changed. This change might be affecting the efficiency of resonance energy transfer from the Tyr to the nearby Trp, the fluorescence quenching by other close chains, or both.

Surface properties of SP-B synthetic peptides

Previous experiments have recently analyzed the surface-tension-reducing properties of different SP-B synthetic

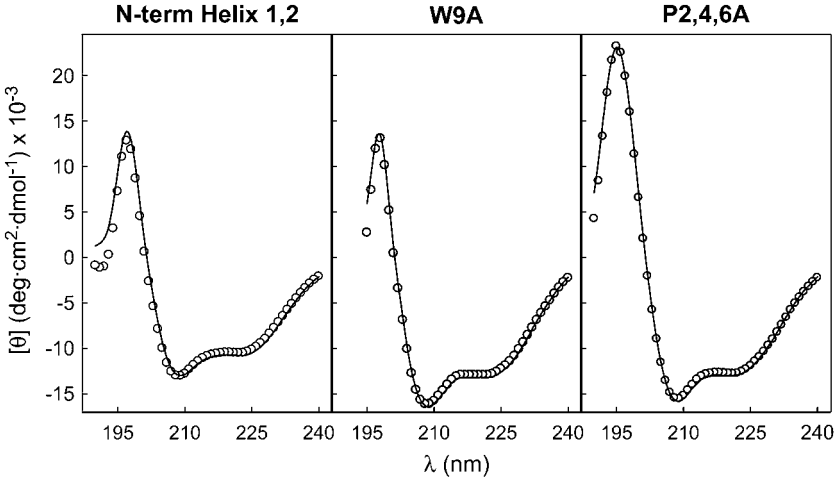

FIGURE 2 Secondary structure of SP-B-derived peptides. Far-UV CD spectra of SP-B synthetic peptides dissolved in methanol at room temperature. Solid lines represent the best fit of the experimental data to theoretical spectra, calculated according to the CDSSTR analysis (22).

TABLE 1 Secondary structure of SP-B synthetic peptides in methanol, estimated from their far-UV CD spectra

	Percentage of secondary structure			
	α-Helix	β-Sheet	β-Turns	Random
N-term Helix 1,2	44 ± 7	11 ± 4	22 ± 3	23 ± 7
W9A	54 ± 5	6 ± 5	21 ± 6	19 ± 4
P2,4,6A	57 ± 6	8 ± 4	19 ± 3	16 ± 6

Note that results are expressed as means ± SD of the estimated values resulting from the analysis of the CD data with three different programs (SELCON 3, CDSSTR, and CONTIN/LL).

peptides reconstituted in DPPC/POPG (7:3, w/w) bilayers in a captive bubble surfactometer (20). Substitution of P2,4,6 or W9 by alanine resulted in significantly increased minimum surface tension (decreased maximum surface pressure) of peptide N-term Helix 1,2 upon cycling. To assess the importance of Trp-9 and Pro-2, -4, and -6 in the surface activity of SP-B-derived synthetic peptides, we have performed different surface experiments in Langmuir balances where the surface pressure-area (π-A) dependencies can be accurately measured during successive cycling of the surface. Cycling rates performed in a Langmuir balance are typically much slower than those occurring during normal respiration but provide detailed information on film properties including dynamic surface-tension-lowering, respreading, compressibility, and hysteresis, allowing a more complete assessment of the surface-active behavior. We first tested the ability of the three SP-B synthetic peptides to adsorb spontaneously to an open air-liquid interface when injected into the buffered aqueous subphase from a methanolic solution (Fig. 4). A rapid increase in surface pressure after peptide injection indicates spontaneous adsorption of the peptide into the interface, as a result of its amphipathic structure. The maximum surface pressure measured in adsorbed peptide monolayers was ~30 mN/m. This maximum pressure was achieved with peptide concentrations of 0.5 μM or higher. Notably, the adsorption rate of the W9A peptide was significantly slower than that of the other two peptides, which adsorbed almost instantaneously. Fig. 4 *d* represents the increase in pressure ($\Pi^{1\text{min}}$) achieved by different peptide concentrations 1 min after injection into the subphase. At these short times, both peptides W9A and P2,4,6A produce substantially lower pressures than the nativelike peptide. Adsorption of peptide W9A requires longer times while peptide P2,4,6A adsorbs apparently as fast as the nativelike sequence, but with an interfacial disposition associated with lower lateral pressures. Fig. 4 *e* plots the final increase in pressure ($\Delta\pi^{20\text{min}}$) reached 20 min after peptide injection. This plot shows how, independently of the adsorption rate, the pressures finally achieved by peptide P2,4,6A are lower than those produced by similar concentrations of the other two peptides, at least for peptide concentrations lower than 0.5 μM in the subphase. Peptide P2,4,6A therefore seems to adopt a different disposition at the interface than the wild-type sequence or the W9A variant.

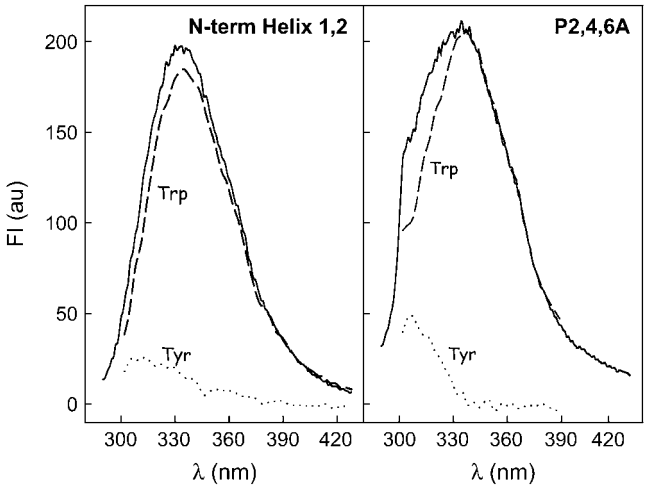

FIGURE 3 Fluorescence of SP-B-derived peptides. Fluorescence emission spectra of SP-B synthetic peptides in methanolic solution. The spectra were obtained upon excitation at 275 nm (*bold line*) and 290 nm (*dashed line*). The spectra obtained upon excitation at 290 nm have been normalized to determine the contribution of Trp to the total fluorescence spectra obtained by excitation at 275 nm. The contribution of Tyr (*dotted line*) was calculated by subtraction of Trp contribution from the total spectrum in each case, as described in Materials and Methods. Peptide concentration was 10 μg/mL.

Peptides N-term Helix 1,2, W9A, and P2,4,6A were also able to perturb and insert into an interface already occupied by a DPPC/POPG (7:3, w/w) monolayer prepared at different initial surface pressures (π_i). In these experiments, the peptides were injected into the subphase underneath a phospholipid monolayer preformed at the interface. Fig. 5 illustrates that injection of any of the three peptides into the subphase underneath the DPPC/POPG monolayer promoted a pressure increase ($\Delta\pi$) as a consequence of the association of the peptide with the interfacial film. The observed $\Delta\pi$ indicated association with, and eventual insertion of, the peptide into the monolayer. Again, the rate of adsorption/insertion of peptide W9A into the phospholipid film was always markedly lower than that of the native sequence or that of the peptide P2,4,6A. In Fig. 6, the increase in surface pressure ($\Delta\pi$) after injection of a given amount of each peptide has been plotted versus the initial surface pressure of the preexisting phospholipid monolayer (π_i). The value $\Delta\pi$ always decreased with increasing π_i for all peptides, as would be expected if tighter lipid packing prevents insertion. From these plots one can calculate the critical insertion pressure (π_c), defined as the maximum pressure at which the peptides are still able to insert. This parameter depends on the monolayer composition as well as on the relative affinity of the peptides to associate with the interface film. It is generally assumed that the lateral packing in a lipid bilayer can be roughly mimicked by a monolayer compressed to ~30 mN/m. Therefore, molecules with π_c values higher than 30 mN/m are generally considered as competent to interact

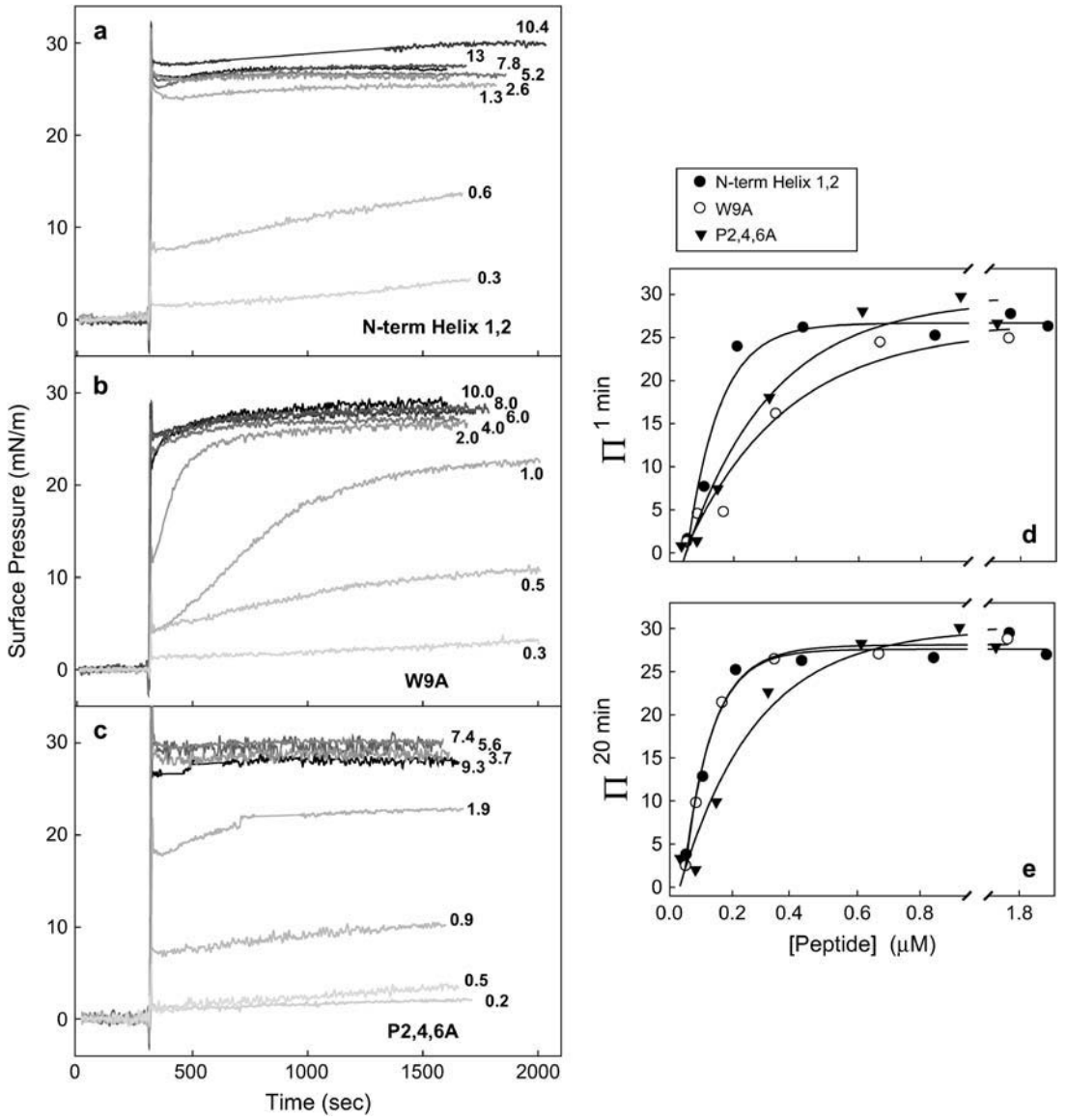

FIGURE 4 Interfacial adsorption of SP-B-derived peptides. (*a–c*) Interfacial adsorption kinetics of SP-B synthetic peptides to a clean air-liquid interface from a buffered subphase (5 mM Tris pH 7, containing 150 mM NaCl). After 5-min equilibration, 10 μL of methanol containing the indicated amounts of peptides (in μg) were injected into the subphase and changes in surface pressure were monitored. The experiments were run at 25°C with continuous stirring of the subphase. Control experiments, performed by injecting the same volume of methanol in the absence of peptide, indicated no significant changes in surface pressure (not shown). (*d*,*e*) Increment of surface pressure 1 min (*d*) or 20 min (*e*) after injection of the different peptides into the subphase, plotted versus peptide concentration.

with and insert into lipid membranes (28). The three SP-B synthetic peptides showed π_c values higher than 30 mN/m, as expected from their ability to perturb lipid bilayers by promoting membrane fusion and lysis (20). The critical pressures calculated for the two substituted variants (40.3 mN/m for W9A and 38.2 mN/m for P2,4,6A) were higher than the π_c obtained for the native sequence (35.4 mN/m).

It is possible that passage through the aqueous hypophase could produce differences in conformation or aggregation state of the peptides that could have consequences in the mode of interaction/insertion with the interfacial monolayer. Potential differences arising from transient exposure of the peptides to a polar environment can be avoided by first mixing lipids and peptide in organic solvents and then spreading the monolayer. Films prepared this way were used to obtain the compression isotherms presented in Fig. 7. The π-A isotherms of DPPC/POPG monolayers are progressively more expanded in the presence of increasing amounts of peptides, indicating that the peptides are also occupying a fraction of the interface. This expansion appears to be greater for the N-term Helix 1,2 peptide than for the two substituted sequences, suggesting that either the native peptide inserted

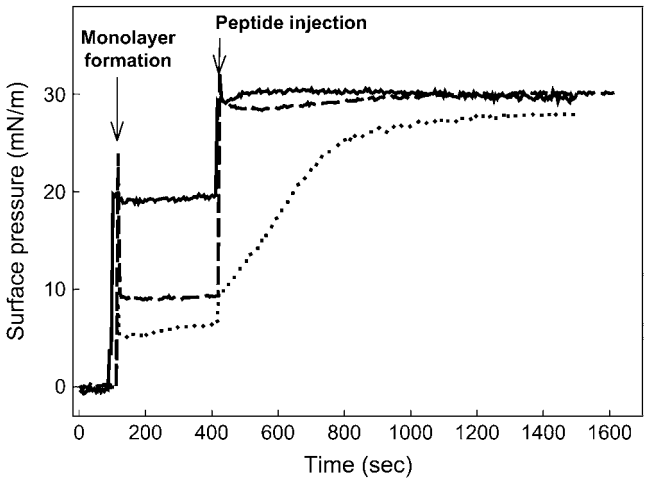

FIGURE 5 Insertion of SP-B-derived peptides into phospholipid monolayers. Representative insertion kinetics experiments of SP-B synthetic peptides injected underneath phospholipid monolayers preformed at different initial surface pressures (π_i). (*Solid line*, N-term Helix 1,2, $\pi_i = 19$ mN/m; *dotted line*, W9A, $\pi_i = 6$ mN/m; and *dashed line*, P2,4,6A, $\pi_i = 9$ mN/m.) The trough was thermostated at 25°C and the subphase was composed of 5 mM Tris buffer pH 7, containing NaCl 150 mM.

into monolayers occupying larger areas, or the number of inserted molecules of this peptide, was higher than the number of molecules of W9A or P2,4,6A peptides. All the three peptides were squeezed-out from the interface at a similar surface pressure, ~50 mN/m, as shown by the convergence of lipid/peptide isotherms with isotherm of pure lipid. Similar squeeze-out pressures have been previously determined for native SP-B purified from animal lungs (29). No additional displacement of the lipid/peptide isotherms was observed beyond the pure lipid isotherm at the highest pressures, indicating that exclusion of the peptide is not accompanied by lipid exclusion. Interestingly, the isotherms of films containing the P2,4,6A peptide present a less marked, if any, squeeze-out plateau than the isotherms of the other two sequences. This fact also suggests that the structural motif more directly involved in the association of this peptide with the interface might have changed as a consequence of Pro substitutions. Peptide P2,4,6A penetrates into the interfacial phospholipid film to a lesser extent, producing a much more limited expansion of the isotherm. At pressures higher than the squeeze-out pressure, isotherms of monolayers containing N-term Helix 1,2 or P2,4,6A peptides do not converge completely, indicating that some peptide remains in the compressed film whereas the W9A peptide seems completely excluded. Again, it seems that the presence of Trp could be the reason for a stronger interaction of N-term Helix 1,2 and P2,4,6A peptides with the interfacial film, resulting in partial retention at higher surface pressures. Although the calculated π_c values suggested that the Trp-containing peptides might be excluded at lower pressures, their high affinity for the interface probably resulted in incomplete removal during rapid compression beyond π_c. This property may also affect the stability of films undergoing compression-expansion cycling. To test this hypothesis, we subjected DPPC/POPG monolayers to several cycles of compression and expansion in the absence or presence of different concentrations of peptides (Fig. 8). In the absence of peptide, only the first compression isotherm reached the highest surface pressure (~70 mN/m), suggesting that the material lost from the compressed phase failed to respread during the subsequent expansion period. In contrast, in the presence of any of the three SP-B synthetic peptides, the isotherms reached the highest pressures even after four compression-expansion cycles. As expected, peptides significantly improved the stability of the film, leading to reproducible curves after several cycles. However, the most interesting feature of isotherms of peptide-containing films may be the presence of conspicuous reinsertion plateaus detected during the expansion periods of the isotherms. These small plateaus, where little change in surface pressure was measured during expansion of the film, are indicative of cooperative reinsertion of surface material previously excluded from the interface. In this context, the isotherms of films containing the peptide with native sequence present much larger reinsertion plateaus than the films containing the two other sequences. This suggests that, at the speed used for expansion (still significantly lower than that imposed by breathing or that employed in the captive bubble surfactometer), N-term Helix 1,2 peptide promoted more efficient reinsertion of material into the interface than W9A or P2,4,6A peptides. We conclude that in addition to peptide affinity for interfaces and peptide stability in compressed phases, the rate of the peptide-promoted reinsertion during

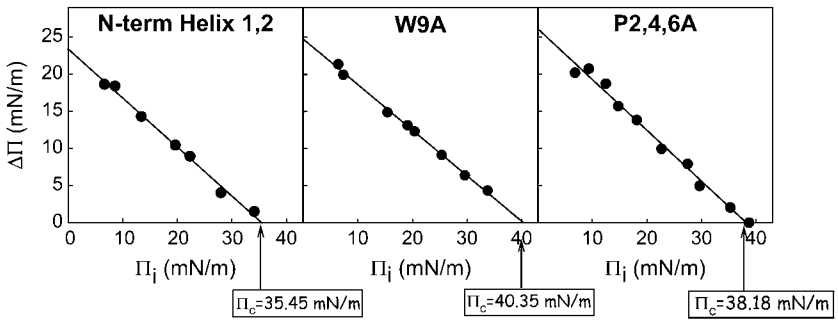

FIGURE 6 Critical pressure for insertion of SP-B-derived peptides in phospholipid films. Increment of surface pressure ($\Delta\pi$) observed in preformed DPPC/POPG (7:3, w/w) monolayers measured 20 min after injection of SP-B synthetic peptides (4 μg) into the subphase, plotted versus the initial surface pressure of the films (π_i). The critical insertion pressure (π_c) was calculated by extrapolation of the plot at $\Delta\pi = 0$ mN/m.

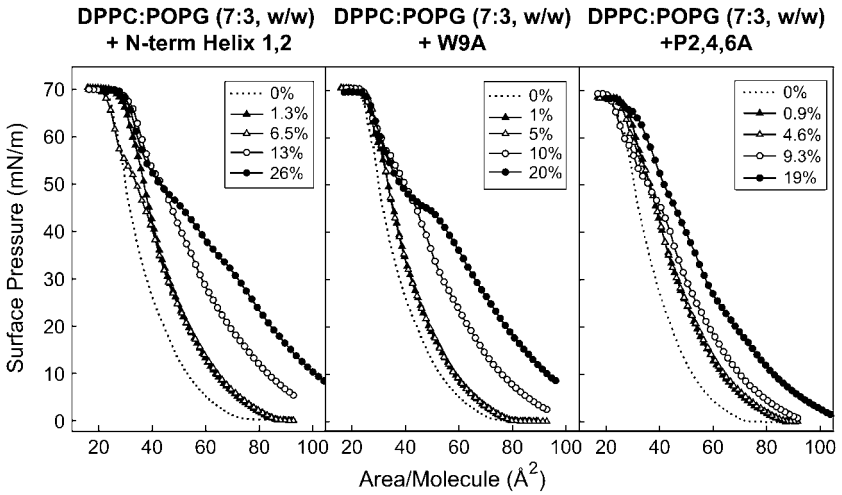

FIGURE 7 Effect of SP-B-derived peptides on the π-A isotherms of lipid/peptide films. Compression isotherms of DPPC/POPG (7:3, w/w) monolayers in the absence or presence of the indicated concentrations of SP-B synthetic peptides (% P/L, w/w).

cycling is also a property of critical importance for efficient surface-film dynamics.

DISCUSSION

Surfactant protein SP-B is a very hydrophobic protein, with an intrinsic amphipathic structure and high capacity for lipid binding. In vitro, SP-B is able to perturb phospholipid vesicles causing lipid mixing, fusion, and lysis (16,18,30,31). It has been also suggested that SP-B may cross-link phospholipid bilayers or bilayers to monolayers (32). These properties may be involved in many of the structural rearrangements of surfactant lipids within the biosynthetic pathway of the type II cell (33) and after secretion of surfactant into the extracellular alveolar airspaces (1,15, 34–36). SP-B plays an essential role in the formation and maintenance of the interfacial film that reduces surface tension and prevents alveolar collapse at end expiration. This

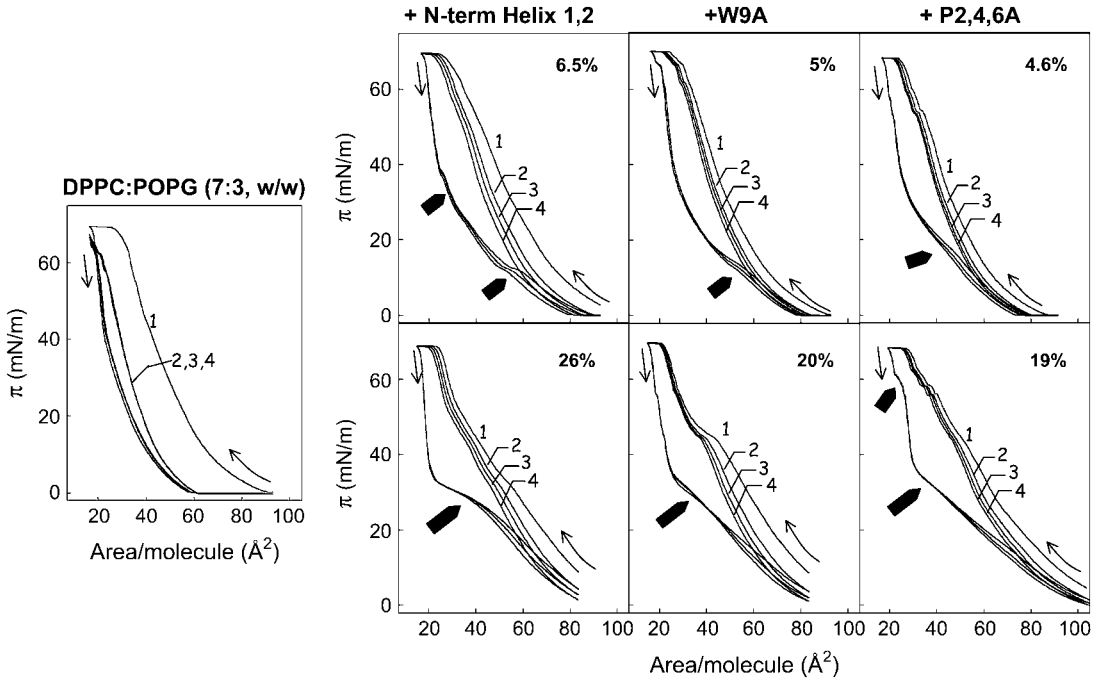

FIGURE 8 Effect of SP-B-derived peptides on cyclic compression-expansion π-A isotherms of lipid and lipid/peptide films. Compression-expansion cyclic isotherm of DPPC/POPG (7:3, w/w) monolayers in the absence (*left panel*) or in the presence (*right panels*) of the indicated concentrations of SP-B synthetic peptides (% P/L, w/w). Films were formed by spreading chloroform/methanol solutions of lipid or lipid and peptide on top of the buffered subphase (Tris 5 mM and NaCl 150 mM, pH 7). After 10-min equilibration, monolayers were compressed and expanded up to four cycles (numbered 1–4), at 25°C, and the changes in surface pressure were registered versus area/phospholipid molecule. Thin arrows indicate the direction at the beginning of the compression and expansion periods. Thick arrows show the regions of the isotherms where reinsertion of material into the monolayer was detected during expansion.

is likely the main reason why SP-B-deficient infants develop fatal respiratory failure shortly after birth (2,37,38). Maintenance of a stable surface film is essential for respiration and requires efficient transfer of phospholipids between the extracellular large aggregate surfactant pool and the air-liquid interface. This process involves rapid insertion of phospholipids into the expanding film during inhalation followed by tight phospholipid packing and partial exclusion from the compressed film during exhalation. SP-B (as well as SP-C) promotes adsorption of phospholipids from vesicles in the aqueous subphase into the air-liquid interface in vitro (29), but the mechanism by which SP-B promotes bilayer-monolayer transitions, and the structural determinants required to achieve this function, are not understood (1,15,36). Recent studies suggest that the hydrophobic surfactant proteins may accelerate adsorption by acting as catalysts that stabilize a high-energy intermediate structure between bilayers and the interfacial film (39,40).

A recent study designed to map essential functional motifs in the sequence of SP-B (20) revealed that a synthetic peptide comprised of amino acids 1–37 of SP-B was able to reproduce reasonably well the fusogenic, lytic, and surface activities of the mature protein. Interestingly, several studies have characterized lipid-protein interactions and surface activity of a peptide from the N-terminal region of SP-B, SP-B (1–25), which mimics many of the biophysical activities of mature SP-B both in vitro (41–44) and in vivo (45). The study by Ryan et al. (20) also showed that the N-terminal tail (residues 1–9) of SP-B is particularly critical for the surface-tension-reducing properties of the protein. For instance, substitution of W9 or Pro-2, -4, and -6, resulted in significant reduction of surface activity without affecting fusogenic or lytic properties. The goal of this study was to determine the structural and functional implications of these two N-terminal motifs, in terms of surface activity.

Table 2 summarizes the different features of the three SP-B peptides with respect to their interfacial properties. The optimal properties of N-term Helix 1,2 (the wild-type-like peptide) indicate that, apart from the ability to perturb the lipid packing of bilayers and monolayers, the capacity to produce very low surface tension upon repetitive compression-expansion cycling requires 1), a very high affinity for the interface; and 2), stable association with the film after compression at relatively high pressure. Very high affinity for the interface is required to rapidly insert the SP-B peptide into the surface film during the brief expansion interlude. The ability to penetrate/perturb films compressed to pressures higher than 40–45 mN/m is probably required for SP-B to promote insertion of phospholipids into the surface film, which probably never gets pressures lower than 45 mN/m in vivo, at the end of inspiration. The ability of the native sequence to sustain pressures within this range may permit a fraction of the protein to remain stably associated with the interface at the highest pressures (lowest tensions).

TABLE 2 Summary of surface activities of SP-B derived peptides

	N-Term Helix 1,2	W9A	P2,4,6A
Rapid absorption to open interfaces	+++	—	++
Insertion into preformed phospholipid films	+++	++	+++
Expansion of lipid/peptide isotherms	+++	++	—
Stable association with compressed films beyond squeeze-out pressure	+++	—	+
Promotion of rapid reinsertion of material during expansion	+++	+	++

Substitution of prolines or tryptophan in the N-terminal segment of SP-B likely produces some structural change in the peptide. The N-terminal segment of SP-B contains an α-helical segment (presumably Helix 1), comprising residues 8–22, in membrane environments, with residues 1–8 forming a β-sheet-like motif (46). Peptides W9A and P2,4,6A variants show increased α-helical content (estimated in Table 1), presumably by N-terminal extension or further stabilization of Helix 1. This conformational rearrangement probably affects the spatial orientation of the N-terminal segment (residues 1–9) with respect to Helix 1, including the relative oriented exposure of aromatic residues Tyr-7 and Trp-9. The modified contribution of Tyr to the fluorescence emission spectra of peptide P2,4,6A would be consistent with such an alteration.

The substitution of tryptophan at position 9 by alanine in peptide W9A resulted in a significant decrease in the rate of adsorption/insertion of the peptide into the expanding interface. Tryptophan residues are known to have a high tendency to locate at membrane interfaces and are among the residues with more favorable free energy to partition into hydrophobic/hydrophilic interfaces (47). The absence of

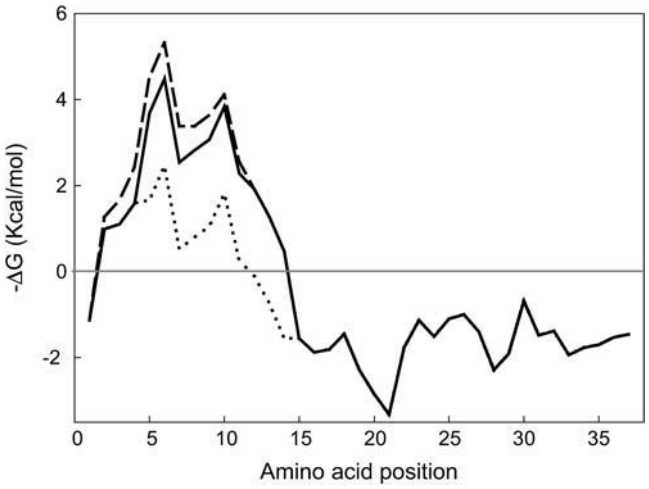

FIGURE 9 Profile of hydrophobicity-at-interface of SP-B-derived peptides. Hydropathy plot of the sequence of SP-B synthetic peptides calculated using the hydrophobic-at-interface scale proposed by Wimley and White (47), where the free energy of transfer of different segments of the protein from a phospholipid bilayer into a water phase is plotted against its position in the sequence. N-term Helix 1,2 (*solid line*), W9A (*dotted line*), and P2,4,6A (*dashed line*).

Trp-9 may therefore affect the propensity of the peptide to adsorb to the air-liquid interface. As a consequence, the peptide is likely progressively lost during successive compression-expansion cycles and the ability to replace lipid molecules excluded from the compressed film is diminished. Moreover, at surface pressures higher than 50 mN/m, the W9A peptide was completely excluded from the interface while N-term Helix 1,2 remained partially attached to it, similar to native SP-B (48,49). These results support the hypothesis that Trp-9 increases the affinity of the peptide for the interface, promotes rapid insertion between phospholipid acyl chains, and stabilizes association with the film at high surface pressures. Previous fluorescence quenching studies indicated that only residues Tyr-7 to Trp-9 in the N-terminal tail of SP-B are fully embedded in the membrane (50). Fig. 9 shows that this is in fact the region within the first half of the

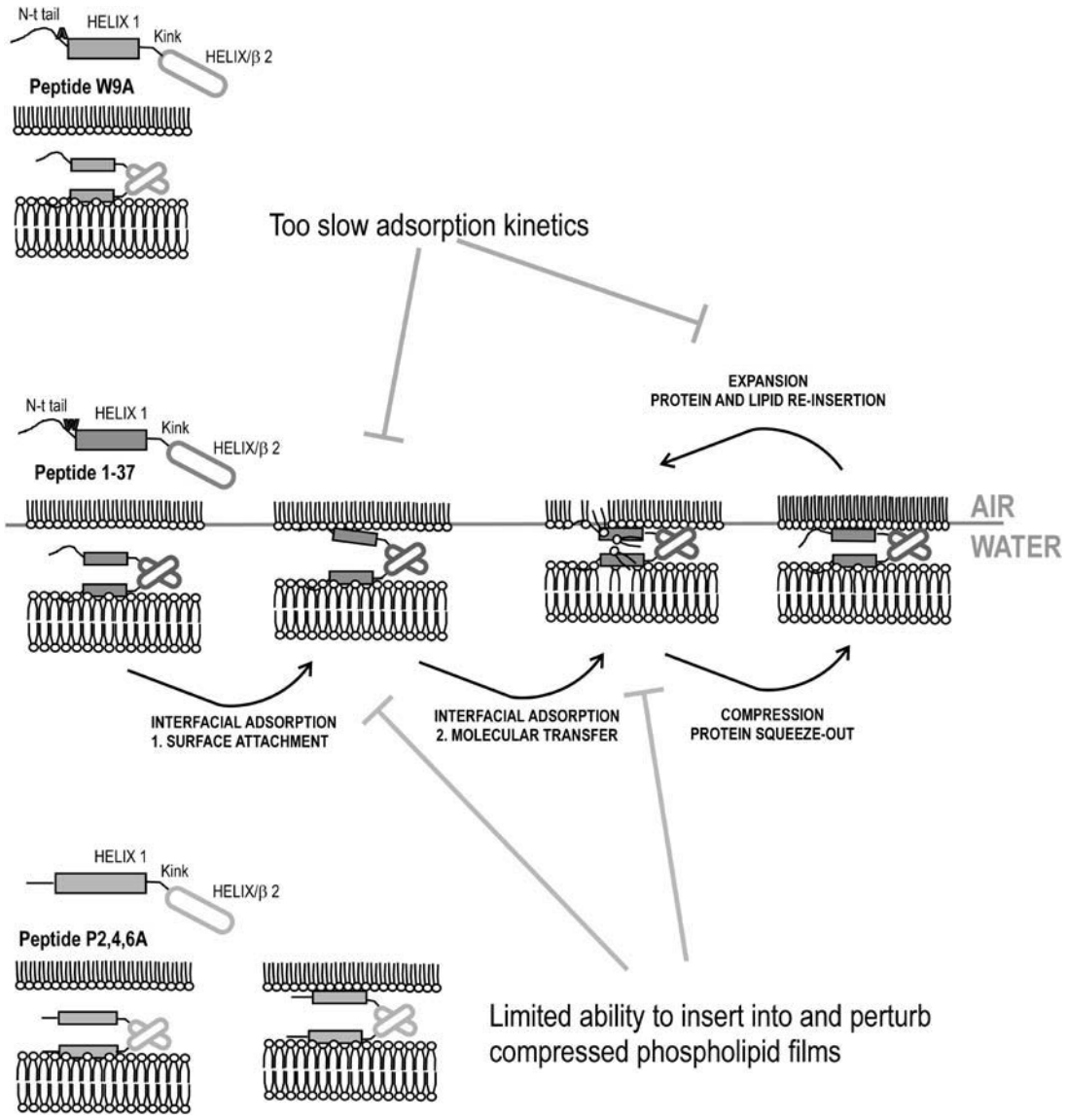

FIGURE 10 Model for the potential molecular mechanisms implied in surface activity of SP-B-derived peptides. Mechanisms potentially implicated in surface activity of peptide N-term Helix 1,2 are depicted in the central scheme. Helix 1 is the main motif that perturbs lipid packing in phospholipid bilayers, but requires the presence of the N-terminal tail (residues 1–9) to insert into and perturb compressed interfacial films. Helix/β2 is a protein-protein interacting motif that facilitates peptide-mediated bilayer-monolayer contacts. Through these contacts, concerted perturbations introduced into both the bilayers (via Helix 1 plus N-terminal tail) and the interfacial film (with the essential participation of the N-terminal tail) would produce efficient transfer of phospholipids into the interface. Compression to the highest pressures (at end expiration) partially excludes the N-terminal tail from interface, followed by reinsertion upon expansion (at inspiration) promoting coinsertion and reextension of associated lipids. Peptide W9A (*top scheme*) would have lower adsorption kinetics producing inefficient interfacial adsorption and reinsertion during expansion. Proline substitution in peptide P2,4,6A (*bottom scheme*) produces a conformational change that extends Helix 1 and eliminates the N-terminal tail motif. Without this motif, the peptide is not able to sufficiently perturb the packing of interfacial films and promote lipid insertion.

SP-B protein that possesses the highest interfacial hydrophobicity. Fig. 9 also illustrates how substitution of Trp-9 by Ala substantially changes the hydropathy profile of the sequence, decreasing the propensity of the N-terminal end of the sequence to partition into membrane interfaces.

The failure of peptide P2,4,6A to generate high surface pressures (lowest tensions) during successive compression-expansion cycling may be related to the diminished ability of this peptide to expand a phospholipid film beyond a certain pressure. This feature is probably related to the conformational change resulting from the substitution of prolines. We speculate that the absence of the helix-breaking prolines promotes a reorientation of the N-terminal segment with respect to the main axis of amphipathic Helix 1, which is constrained to follow the membrane plane. This change in orientation probably produces a slight change in the environment of the aromatic residues, Trp-9 and Tyr-7. This hypothesis has been already proposed by others based on topographical studies of a smaller SP-B-derived synthetic peptide, SP-$B_{1\text{-}25}$ (50). Peptide P2,4,6A showed relatively rapid adsorption to the interface, likely as a consequence of the presence of the two aromatic residues, but once there, penetrated into the interface to a lesser extent than proline-containing sequences. As illustrated in the scheme depicted in Fig. 10, the parallel disposition of amphipathic Helix 1 at the polar surface of the phospholipid film probably imposes restrictions on the orientation of the N-terminal tail (residues 1–9). Prolines 2, 4, and 6 would promote proper orientation of aromatic residues that penetrate into the interface and produce an important increase in surface pressure. Penetration of the peptide into the hydrophobic interfacial region might be important to provide enough packing distortion for the film to accommodate new lipid molecules during interfacial adsorption or reinsertion. A similar model was recently proposed by Wang and co-workers (50), who suggested that the orientation of the N-terminal prolines in the membrane might be influenced by the conformation of the next few residues before the α-helix, Tyr-7, Cys-8, and Trp-9. According to their theoretical analysis, if these residues adopt a α-helical conformation, the side chain of Trp-9 would be exposed to the solvent instead of fully embedded in the phospholipid membrane. In this case, interaction of the peptide with phospholipids would likely be impaired and surface activity decreased.

Fig. 10 integrates the current findings into a model that illustrates how the structure of SP-B might facilitate the surface-tension-reducing properties of the peptide. We have previously shown that the N-terminal half of the protein, including residues 1–37, contains all the determinants required to promote fusion and lysis of membranes as well as to produce and sustain very low surface tensions (20). The importance of the N-terminal region for the function of SP-B has been suggested by other authors (20,41–44,50,51). We speculate that this domain contains most of the membrane-interacting motifs in SP-B, whereas the C-terminal half could perhaps be involved instead in protein-protein interactions, either within the native SP-B dimer or within higher-order oligomers. Helix 1 contains the main membrane-perturbing motif, and its ability to perturb lipid packing in surfactant bilayers is probably required to extract lipid molecules from subphase membranes for insertion into the air-liquid interface. Saposins, a family of proteins structurally homologous to SP-B (9), have a similar activity, i.e., extracting lipid molecules—in this case sphingolipids—from membranes to facilitate their catalysis by sphingolipidases. In the case of SP-B, phospholipid molecules extracted from surfactant bilayers would be targeted to the interfacial film. We have proposed that the motif we previously termed *Helix 2* could promote peptide-peptide interactions that bring into close proximity two bilayers (required for SP-B to catalyze lipid exchange or fusion between vesicles) or a bilayer and the interfacial monolayer (to catalyze interfacial adsorption or reinsertion) (20). Consistent with this model, only peptides containing the *Helix 2* motif, produced agglutination of both Gram+ and Gram− bacteria (unpublished data). A study by Flach et al. (26), of the structure of a SP-B peptide (9–36) in methanol, assigned an antiparallel β-sheet conformation to the segment 26–32. Such β-sheet conformation would contradict the model proposed in Fig. 1. One possibility is that peptide 1–37, as the 9–36 peptide studied by Flach et al. (26), might have a tendency to fold into β-sheet instead of α-helix when it is isolated from the structural context of the whole protein. This tendency could promote peptide-peptide interactions that mediate peptide self-association and bilayer-bilayer or bilayer-monolayer apposition. Interestingly, peptide SP-B (1–25), which lacks the *Helix 2* motif, significantly improved surface properties when it is synthesized as a dimeric form (52). Adoption of β-sheet instead of α-helical conformation in at least a fraction of the peptides could also explain the proportion of secondary structure determined for the different peptide variants in methanol (in Table 1). On the other hand, Helix 1 alone would not be sufficient to insert into and perturb interfacial phospholipid films at surface pressures higher than those existing in free standing bilayers (~30 mN/m). The results of this work suggest that the N-terminal tail of SP-B has been specially optimized to insert rapidly into and maintain association with highly packed surface films. This motif promotes very rapid and efficient insertion-exclusion-reinsertion kinetics during the respiratory compression-expansion cycle, and should be necessarily considered when designing SP-B mimic peptides.

REFERENCES

1. Pérez-Gil, J., A. Cruz, and I. Plasencia. 2005. Structure-function relationships of hydrophobic surfactant proteins SP-B and SP-C in pulmonary surfactant. *In* Developments in Lung Surfactant (Dys)-Function. K. E. Nag, editor. Marcel Dekker, New York.
2. Nogee, L. M., G. Garnier, H. C. Dietz, L. Singer, A. M. Murphy, D. E. deMello, and H. R. Colten. 1994. A mutation in the surfactant protein B gene responsible for fatal neonatal respiratory disease in multiple kindreds. *J. Clin. Invest.* 93:1860–1863.

3. Clark, J. C., S. E. Wert, C. J. Bachurski, M. T. Stahlman, B. R. Stripp, T. E. Weaver, and J. A. Whitsett. 1995. Targeted disruption of the surfactant protein B gene disrupts surfactant homeostasis, causing respiratory failure in newborn mice. *Proc. Natl. Acad. Sci. USA*. 92: 7794–7798.

4. Glasser, S. W., M. S. Burhans, T. R. Korfhagen, C. L. Na, P. D. Sly, G. F. Ross, M. Ikegami, and J. A. Whitsett. 2001. Altered stability of pulmonary surfactant in SP-C-deficient mice. *Proc. Natl. Acad. Sci. USA*. 98:6366–6371.

5. Melton, K. R., L. L. Nesslein, M. Ikegami, J. W. Tichelaar, J. C. Clark, J. A. Whitsett, and T. E. Weaver. 2003. SP-B deficiency causes respiratory failure in adult mice. *Am. J. Physiol. Lung Cell. Mol. Physiol*. 285:L543–L549.

6. Lewis, J. F., and R. Veldhuizen. 2003. The role of exogenous surfactant in the treatment of acute lung injury. *Annu. Rev. Physiol*. 65: 613–642.

7. Gregory, T. J., W. J. Longmore, M. A. Moxley, J. A. Whitsett, C. R. Reed, A. A. Fowler 3rd, L. D. Hudson, R. J. Maunder, C. Crim, and T. M. Hyers. 1991. Surfactant chemical composition and biophysical activity in acute respiratory distress syndrome. *J. Clin. Invest*. 88:1976–1981.

8. Munford, R. S., P. O. Sheppard, and P. J. O'Hara. 1995. Saposin-like proteins (SAPLIP) carry out diverse functions on a common backbone structure. *J. Lipid Res*. 36:1653–1663.

9. Liepinsh, E., M. Andersson, J. M. Ruysschaert, and G. Otting. 1997. Saposin fold revealed by the NMR structure of NK-lysin. *Nat. Struct. Biol*. 4:793–795.

10. Cruz, A., C. Casals, and J. Perez-Gil. 1995. Conformational flexibility of pulmonary surfactant proteins SP-B and SP-C, studied in aqueous organic solvents. *Biochim. Biophys. Acta*. 1255:68–76.

11. Pastrana-Rios, B., S. Taneva, K. M. Keough, A. J. Mautone, and R. Mendelsohn. 1995. External reflection absorption infrared spectroscopy study of lung surfactant proteins SP-B and SP-C in phospholipid monolayers at the air/water interface. *Biophys. J*. 69:2531–2540.

12. Pérez-Gil, J., C. Casals, and D. Marsh. 1995. Interactions of hydrophobic lung surfactant proteins SP-B and SP-C with dipalmitoylphosphatidylcholine and dipalmitoylphosphatidylglycerol bilayers studied by electron spin resonance spectroscopy. *Biochemistry*. 34: 3964–3971.

13. Cruz, A., L. Vazquez, M. Velez, and J. Perez-Gil. 2004. Effect of pulmonary surfactant protein SP-B on the micro- and nanostructure of phospholipid films. *Biophys. J*. 86:308–320.

14. Andersson, M., T. Curstedt, H. Jornvall, and J. Johansson. 1995. An amphipathic helical motif common to tumourolytic polypeptide NK-lysin and pulmonary surfactant polypeptide SP-B. *FEBS Lett*. 362:328–332.

15. Pérez-Gil, J. 2001. Lipid-protein interactions of hydrophobic proteins SP-B and SP-C in lung surfactant assembly and dynamics. *Pediatr. Pathol. Mol. Med*. 20:445–469.

16. Poulain, F. R., L. Allen, M. C. Williams, R. L. Hamilton, and S. Hawgood. 1992. Effects of surfactant apolipoproteins on liposome structure: implications for tubular myelin formation. *Am. J. Physiol*. 262:L730–L739.

17. Poulain, F. R., S. Nir, and S. Hawgood. 1996. Kinetics of phospholipid membrane fusion induced by surfactant apoproteins A and B. *Biochim. Biophys. Acta*. 1278:169–175.

18. Oosterlaken-Dijksterhuis, M. A., M. van Eijk, L. M. van Golde, and H. P. Haagsman. 1992. Lipid mixing is mediated by the hydrophobic surfactant protein SP-B but not by SP-C. *Biochim. Biophys. Acta*. 1110:45–50.

19. Schürch, S., F. H. Green, and H. Bachofen. 1998. Formation and structure of surface films: captive bubble surfactometry. *Biochim. Biophys. Acta*. 1408:180–202.

20. Ryan, M. A., X. Qi, A. G. Serrano, M. Ikegami, J. Perez-Gil, J. Johansson, and T. E. Weaver. 2005. Mapping and analysis of the lytic and fusogenic domains of surfactant protein B. *Biochemistry*. 44: 861–872.

21. Ruano, M. L., I. Garcia-Verdugo, E. Miguel, J. Perez-Gil, and C. Casals. 2000. Self-aggregation of surfactant protein A. *Biochemistry*. 39:6529–6537.

22. Sreerama, N., and R. W. Woody. 2000. Estimation of protein secondary structure from circular dichroism spectra: comparison of CONTIN, SELCON, and CDSSTR methods with an expanded reference set. *Anal. Biochem*. 287:252–260.

23. Sreerama, N., and R. W. Woody. 2004. On the analysis of membrane protein circular dichroism spectra. *Protein Sci*. 13:100–112.

24. Nuñez, E., X. Wei, C. Delgado, I. Rodriguez-Crespo, B. Yelamos, J. Gomez-Gutierrez, D. L. Peterson, and F. Gavilanes. 2001. Cloning, expression, and purification of histidine-tagged preS domains of hepatitis B virus. *Protein Expr. Purif*. 21:183–191.

25. Serrano, A. G., A. Cruz, K. Rodriguez-Capote, F. Possmayer, and J. Perez-Gil. 2005. Intrinsic structural and functional determinants within the amino acid sequence of mature pulmonary surfactant protein SP-B. *Biochemistry*. 44:417–430.

26. Flach, C. R., P. Cai, D. Dieudonne, J. W. Brauner, K. M. Keough, J. Stewart, and R. Mendelsohn. 2003. Location of structural transitions in an isotopically labeled lung surfactant SP-B peptide by IRRAS. *Biophys. J*. 85:340–349.

27. Lakowicz, J. R. 1999. Principles of Fluorescence Spectroscopy. Plenum Press, New York. 445–486.

28. Brockman, H. 1999. Lipid monolayers: why use half a membrane to characterize protein-membrane interactions? *Curr. Opin. Struct. Biol*. 9:438–443.

29. Cruz, A., L. A. Worthman, A. G. Serrano, C. Casals, K. M. Keough, and J. Perez-Gil. 2000. Microstructure and dynamic surface properties of surfactant protein SP-B/dipalmitoylphosphatidylcholine interfacial films spread from lipid-protein bilayers. *Eur. Biophys. J*. 29:204–213.

30. Chang, R., S. Nir, and F. R. Poulain. 1998. Analysis of binding and membrane destabilization of phospholipid membranes by surfactant apoprotein B. *Biochim. Biophys. Acta*. 1371:254–264.

31. Creuwels, L. A., L. M. van Golde, and H. P. Haagsman. 1996. Surfactant protein B: effects on lipid domain formation and intermembrane lipid flow. *Biochim. Biophys. Acta*. 1285:1–8.

32. Zaltash, S., M. Palmblad, T. Curstedt, J. Johansson, and B. Persson. 2000. Pulmonary surfactant protein B: a structural model and a functional analogue. *Biochim. Biophys. Acta*. 1466:179–186.

33. Weaver, T. E. 1998. Synthesis, processing and secretion of surfactant proteins B and C. *Biochim. Biophys. Acta*. 1408:173–179.

34. Whitsett, J. A., and T. E. Weaver. 2002. Hydrophobic surfactant proteins in lung function and disease. *N. Engl. J. Med*. 347:2141–2148.

35. Weaver, T. E., and J. J. Conkright. 2001. Function of surfactant proteins B and C. *Annu. Rev. Physiol*. 63:555–578.

36. Pérez-Gil, J., and K. M. Keough. 1998. Interfacial properties of surfactant proteins. *Biochim. Biophys. Acta*. 1408:203–217.

37. Nogee, L. M., D. E. de Mello, L. P. Dehner, and H. R. Colten. 1993. Brief report: deficiency of pulmonary surfactant protein B in congenital alveolar proteinosis. *N. Engl. J. Med*. 328:406–410.

38. deMello, D. E., S. Heyman, D. S. Phelps, A. Hamvas, L. Nogee, S. Cole, and H. R. Colten. 1994. Ultrastructure of lung in surfactant protein B deficiency. *Am. J. Respir. Cell Mol. Biol*. 11:230–239.

39. Schram, V., and S. B. Hall. 2001. Thermodynamic effects of the hydrophobic surfactant proteins on the early adsorption of pulmonary surfactant. *Biophys. J*. 81:1536–1546.

40. Schram, V., and S. B. Hall. 2004. SP-B and SP-C alter diffusion in bilayers of pulmonary surfactant. *Biophys. J*. 86:3734–3743.

41. Bruni, R., H. W. Taeusch, and A. J. Waring. 1991. Surfactant protein B: lipid interactions of synthetic peptides representing the amino-terminal amphipathic domain. *Proc. Natl. Acad. Sci. USA*. 88:7451–7455.

42. Gordon, L. M., S. Horvath, M. L. Longo, J. A. Zasadzinski, H. W. Taeusch, K. Faull, C. Leung, and A. J. Waring. 1996. Conformation and molecular topography of the N-terminal segment of surfactant

protein B in structure-promoting environments. *Protein Sci.* 5:1662–1675.

43. Lipp, M. M., K. Y. Lee, J. A. Zasadzinski, and A. J. Waring. 1996. Phase and morphology changes in lipid monolayers induced by SP-B protein and its amino-terminal peptide. *Science*. 273:1196–1199.
44. Longo, M. L., A. M. Bisagno, J. A. Zasadzinski, R. Bruni, and A. J. Waring. 1993. A function of lung surfactant protein SP-B. *Science*. 261:453–456.
45. Gupta, M., J. M. Hernandez-Juviel, A. J. Waring, and F. J. Walther. 2001. Function and inhibition sensitivity of the N-terminal segment of surfactant protein B (SP-B1–25) in preterm rabbits. *Thorax*. 56: 871–876.
46. Gordon, L. M., K. Y. Lee, M. M. Lipp, J. A. Zasadzinski, F. J. Walther, M. A. Sherman, and A. J. Waring. 2000. Conformational mapping of the N-terminal segment of surfactant protein B in lipid using 13C-enhanced Fourier-transform infrared spectroscopy. *J. Pept. Res.* 55: 330–347.
47. Wimley, W. C., and S. H. White. 1996. Experimentally determined hydrophobicity scale for proteins at membrane interfaces. *Nat. Struct. Biol.* 3:842–848.
48. Nag, K., S. G. Taneva, J. Perez-Gil, A. Cruz, and K. M. Keough. 1997. Combinations of fluorescently labeled pulmonary surfactant proteins SP-B and SP-C in phospholipid films. *Biophys. J.* 72:2638–2650.
49. Putz, G., M. Walch, M. Van Eijk, and H. P. Haagsman. 1999. Hydrophobic lung surfactant proteins B and C remain associated with surface film during dynamic cyclic area changes. *Biochim. Biophys. Acta*. 1453:126–134.
50. Wang, Y., K. M. Rao, and E. Demchuk. 2003. Topographical organization of the N-terminal segment of lung pulmonary surfactant protein B (SP-B(1–25)) in phospholipid bilayers. *Biochemistry*. 42: 4015–4027.
51. Kandasamy, S. K., and R. G. Larson. 2005. Molecular dynamics study of the lung surfactant peptide SP-B1–25 with DPPC monolayers: insights into interactions and peptide position and orientation. *Biophys. J.* 88:1577–1592.
52. Veldhuizen, E. J., A. J. Waring, F. J. Walther, J. J. Batenburg, L. M. van Golde, and H. P. Haagsman. 2000. Dimeric N-terminal segment of human surfactant protein B (dSP-B(1–25)) has enhanced surface properties compared to monomeric SP-B(1–25). *Biophys. J.* 79: 377–384.